ISSN 1028-334X, Doklady Earth Sciences, 2022, Vol. 503, Part 2, pp. 164–167. © Pleiades Publishing, Ltd., 2022.
Russian Text © The Author(s), 2022, published in Doklady Rossiiskoi Akademii Nauk. Nauki o Zemle, 2022, Vol. 503, pp. 37–41.

MINERALOGY

The Crystal Structure of Vyalsovite $FeCaAlS(OH)_5$: First Example of the Commensurate Combination of Iron Sulfide and Hydroxide Layers

S. V. Soboleva[a], N. M. Boeva[a,*], T. E. Evstigneeva[a], and Academician N. S. Bortnikov[a]

Received November 16, 2021; revised December 27, 2021; accepted December 28, 2021

Abstract—Using selected aeria difraction and X-ray powder data, a structural model was constructed for the rare mineral vyalsovite $FeCaAlS(OH)_5$. Parameters of the elementary monoclinic cell *a* 5.205, *b* 21.402, *c* 14.400 Å, β 95°, sp. gr. C_m. The crystal structure of vyalsovite is the first example of a hybrid structure composed of commensurate iron sulfide and hydroxide modules.

Keywords: vyalsovite, crystal structure, commensurate combination, sulfide and hydroxide layers
DOI: 10.1134/S1028334X22040171

INTRODUCTION

In nature there are minerals consisting of modules with different compositions and structures (e.g., sulfide and hydroxide layers); therefore, such structures are commonly referred to as modulated [1]. This class of crystal structures includes the structures of valleriite $(Fe^{2+},Cu)_4(Mg,Al)_3S_4(OH)_6$, tochilinite $Fe^{2+}_{5-6}(Mg,Fe^{2+})_5S_6(OH)_{10}$, ferrotochilinite $Fe^{2+}_6(Fe^{2+},Mg)_5S_6(OH)_{10}$, and some inorganic compounds [2–4]. Since Fe atoms of most sulfides are arranged in tetrahedral coordination, the sulfide and hydroxide components are characterized by noncommensurate sublattices, which is reflected in the complex X-ray powder patterns with overlapping reflexes and microdiffraction images with the sets of reflections corresponding to the various commensurate sublattices.

We describe the first example of the modulated crystal structure consisting of commensurate sulfide and hydroxide modules, which was revealed for vyalsovite $FeCaAlS(OH)_5$.

This mineral was discovered in 1989; its crystal structure was assumed to combine its components, such as $Al(OH)_3$, $Ca(OH)_2$, and FeS [5]. It was named after L.N. Vyal'sov, an eminent specialist in reflected light optics, who studied the unique optical properties of this mineral.

Vyalsovite is an extremely rare hydrosulfide, which has been known until recently only at the place where it was found for the first time at the Komsomolsk Cu–Ni–PGE deposit in the Norilsk region. The mineral was discovered as assemblages and veins of very fine grains from 5–10 to 100–150 μm in size in forsterite skarns in the lower contact zone of the Talnakh gabbro-dolerite intrusion and Devonian dolomites. It is closely associated with the spinel assemblages and is formed together with valleriite, diaspore, djerfisherite, serpentinite, and magnetite, replacing chalcopyrite, forsterite, and spinel [5]. The discoverers [5] presented the results of energy-dispersive analysis, X-ray powder diffraction, and transmission electron microscopy (including microdiffraction), which serve as the basis for deriving its formula $FeCaAlS(OH)_5$ and the unit cell parameters: $a = 14.20$, $b = 20.98$, and $c = 5.496$ Å.

The crystal structure of this mineral remained unknown since material suitable for its study could not be found. Due to new studies of the mineral from a typical sample kept at the Institute of Geology of Ore Deposits, Petrography, Mineralogy, and Geochemistry, Russian Academy of Sciences (Moscow), by precision methods, a model for the vyalsovite crystal structure was developed based on the octahedral coordination of constituent atoms.

MATERIALS AND METHODS

X-ray (Siemens D-500 X-ray powder diffractometer (Cu*K*α-radiation, scanning interval of 2°–70° 2θ)), electron-microscopic (Philips CM12 transmission electron microscope (TEM) with an EDAX 9800 attachment), and simultaneous-thermal (STA) (Netzsch 449 F1 Jupiter STA instrument) analyses were used. To refine the crystal structure, we

[a] *Institute of Geology of Ore Deposits, Petrography, Mineralogy, and Geochemistry, Russian Academy of Sciences, Moscow, 119017 Russia*
**e-mail: boeva@igem.ru*

Table 1. Experimental and calculated values of intensities and *d*-spacings *d*(*hkl*) for the X-ray powder pattern of vyalsovite

I (exp)	*I* (calc)	*d* (exp)	*d* (calc)	*hkl*
58	50	10.65	10.70	020
100	100	5.40	5.35	040
8	6	3.590	3.586	$00\bar{4}$
8	8	3.389	3.400	$02\bar{4}$
5	4	3.000	3.063	$15\bar{4}$
10	10	2.910	2.978, 2.9362	152
10	7	2.688	2.675	080
20	16	2.500	2.528, 2.507	$06\bar{4}$, $17\bar{2}$
15	15	2.302	2.3331	204
15	10	2.260	2.264	173
40	30	2.150	2.148, 2.144	$22\bar{4}$, $08\bar{4}$
8	5	2.079	2.090	$19\bar{2}$
20	20	1.978	1.983	224
15	12	1.886	1.880, 1.871	156, $26\bar{4}$
20	18	1.850	1.859, 1.840	280, $0.10.\bar{4}$
18	15	1.781	1.790, 1.783	0.12.0
10	10	1.715	1.700	157
10	6	1.675	1.678	330
8	5	1.650	1.644	$1.11.\bar{4}$
10	6	1.595	1.591	$35\bar{2}$
10	7	1.525	1.531, 1.528	$2.10.\bar{4}$, 0.14.0
8	5	1.485	1.489, 1.480	217
5	5	1.405	1.400	$39\bar{1}$
5	5	1.345	1.343	316

employed a theoretical method for modeling using the ATOMS and CARINE software that enabled us to control the interatimic distances in the different coordination environments around cations and to estimate the diffraction characteristics (the data of X-ray powder patterns and microdiffraction images) corresponding to the different models.

RESULTS

According to the data of the X-ray powder pattern (Table 1) and the microdiffraction image (Fig. 1), we determined a C-centered monoclinic unit cell with parameters $a = 5.205$, $b = 21.402$, $c = 14.400$ Å, $\beta = 95°$, $Z = 8$, $d(\text{calc}) = 2.00$. Space group C1m1 was selected by the character of distribution of the reflex intensity along the series of *hk*0.

These values are similar to the values in [5], being different, however, in the selection of axes. The C-centered orthorhombic crystal system proposed [5] does not correspond to the microdiffraction image in Fig. 1, which suits the requirement $h + k = 2n$ and clearly demonstrates an excess by nearly four times of *d*(020) (~20 Å) compared to *d*(200) (~5 Å).

The X-ray powder pattern shows a good agreement between the experimental and theoretical values of interplanar spacings *d*(*hkl*) and the intensities of reflexes (Table 1). Some disagreements with the data of the X-ray powder pattern presented in [5] are caused by the different conditions of imaging: a Gandolfi camera and an approximate evaluation of the reflex intensities using calibration marks. The intensities of reflections in the microdiffraction image also agree well with the theoretical data, in particular, the reflection intensity (040) clearly exceeds the reflection intensity (020) by a factor of two.

The presence of a brucite component and a hydroxyl group in the mineral is confirmed by the thermal studies. The endothermal effect with the maximum at $T = 324°C$ points to the destruction of brucite-like layers in the mineral. The endothermal effect in the temperature range of 400–500°C indicates the removal of Ca-related hydroxyl groups. Their loss upon heating was 18.4 wt %, which is close to the theoretical value of 18.77 wt % calculated using the chemical formula.

DISCUSSION

All components, $Al(OH)_3$, $Ca(OH)_2$, and FeS constituting vyalsovite are known as minerals distributed differently in the natural environment. Among them $Al(OH)_3$ corresponds to the formula of gibbsite, the main ore-forming mineral of bauxites, being the weathering products of aluminosilicate rocks. The component $Ca(OH)_2$ is the formula of rare portlandite, which occurs in all types of geological settings both as spheroidal precipitates composed of finely dispersed crystallites and as small perfect crystals. The first find of portlandite is confined to metamorphosed calcium-silicate rocks [6]. Portlandite was also found in the fumarole sediments in the Vesuvius area [7] and in the sedimentary rocks of Jebel-Avke massif, Oman [8]. In the Chelyabinsk coal basin, portlandite is formed during the spontaneous combustion of coal seams [9]. A synthetic analog of portlandite $Ca(OH)_2$ is a base for the cement component due to the tendency towards rapid decomposition with water loss and the transition to CaO oxide, which is strong and resistant to different impacts. Finally, the FeS component is known as a rare mineral troilite, discovered in association with olivine, chromite, graphite, and a series of phosphate minerals in several meteorites that originated from the Moon or Mars [10]. However, one of the recent findings of troilite was in the Chelyabinsk meteorite that fell into Chebarkul Lake (Chelyabinsk oblast) in February 2013 [11]. Troilite is considered to

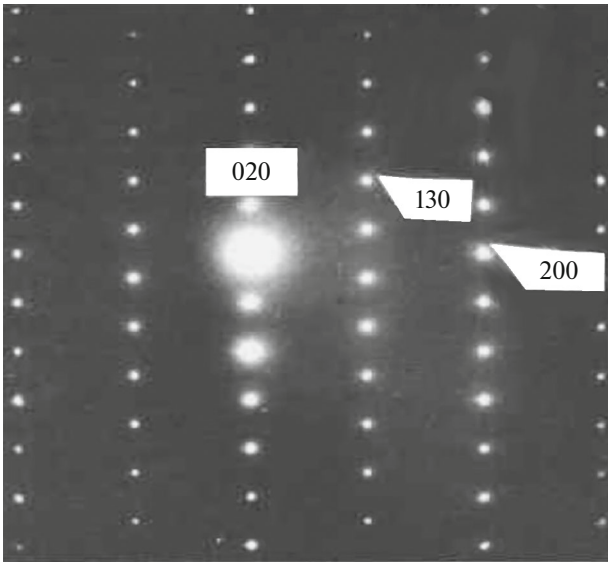

Fig. 1. Microdiffraction image (similar to Fig. 5 from [5] with corrected indices of reflexes) demonstrating the C-centered lattice along the (001) plane.

be an important component of lunar soil. Troilite was discovered in the Rustenburg Pt deposit in close association with the Pt–Fe alloy, pyrrhotine, secondary hydrous silicates, magnetite, and calcite [12]. The close intergrowths of troilite with hexagonal and monoclinic modifications of pyrrhotine were recorded in serpentine rocks from the Hannover deposit, New Mexico [13].

The crystal structures of these minerals contain layers built of octahedra linked by edges in gibbsite and portlandite and by faces in troilite. The gibbsite structure [14] is formed of single octahedral layers, in which octahedra are occupied by Al^{3+} cations only by 2/3 (so-called dioctahedral layers). The crystal structure of portlandite [15] consists of single octahedral layers and is identical to such of brusite. The weak van-der-Waals bonds between the layers determine the finely dispersed character of the precipitation of these minerals.

In contrast to the structures of gibbsite and portlandite, the structure of troilite is composed of more dense octahedral layers, in which octahedra are linked not by edges but by faces, which leads to structural instability as a result of strong repulsion of Fe^{2+} cations through the common edges of the octahedra. In the crystal structure of troilite from the lunar soil [16], the Fe–S interatomic distances differ considerably from 2.36 to 2.72 Å. In the structure of synthetic FeS [17], the octahedra around Fe atoms are regular, and all the Fe–S distances are equal to 2.49 Å.

A favorable factor for the construction of the vyalsovite structural model was the octahedral coordination of all atoms comprising the crystal structure. This made it possible to arrange the octahedral layers

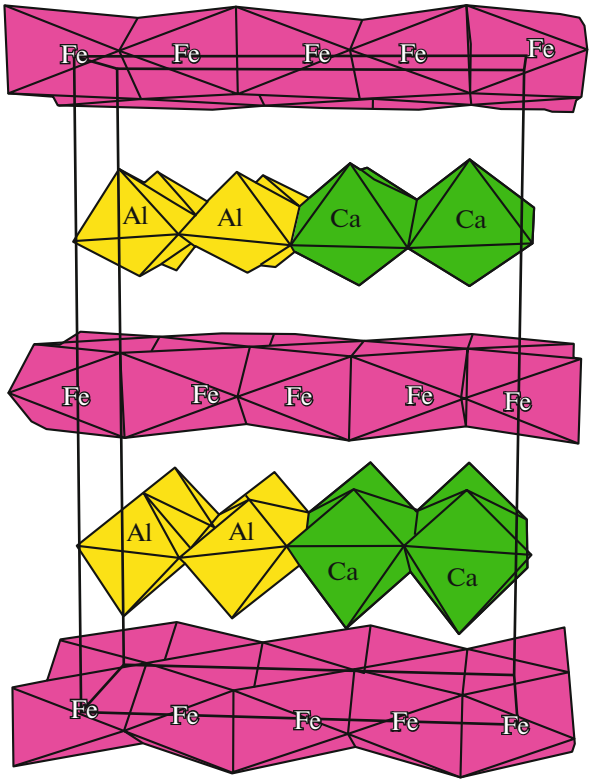

Fig. 2. Model of the vyalsovite crystal structure.

parallel to the (010) plane with alteration of sulfide and hydroxide layers along the longest translation of *b*. The ordered alteration of the octahedral layers of FeS, $Ca(OH)_2$, and $Al(OH)_3$ could be the most likely crystal-chemical model; however, the symmetry *Cm* that implies the translation of $x + 1/2$, $y + 1/2$, does not allow placing two hydroxide layers between the sulfide layers.

Therefore, we proposed a model with one hydroxide layer, consisting of alternating octahedra settled orderly by Ca^{2+} and Al^{3+} cations (Fig. 2). Such an ordered arrangement of the cations with different charges is known in the structures of some titanosilicates: in bornemanite $BaNa_3\{(Na,Ti)_4[(Ti,Nb)_2O_2Si_4O_{14}](F,OH)_2\}PO_4$ [18] and lomonosovite $Na_{10}Ti_2(Nb,Fe,Ti)_2(Si_2O_7)_2(PO_4)_2O_4$ [19], Na^+ and Ti^{4+} cations alternate in an orderly manner in the octahedral layers (in lomonosovite, the Ti^{4+} cation is partially replaced by the Nb^{5+} cation). In the structure of nafertistite $(Na,K)_3(Fe^{2+},Fe^{3+},Mg)_{10}[Ti_2(Si,Fe^{3+},Al)_{12}O_{37}](OH,O)_6$ [20], octahedra are occupied in an orderly way by Ti^{4+} and (Fe^{2+} and Mn^{2+}) cations.

FeS sulfide is a rare example of iron sulfide with octahedral coordination of Fe (Fig. 3); therefore, we suggest a structure of alternating octahedral layers for the mineral vyalsovite.

The Fe–S interatomic distances in the sulfide layers are 2.13–2.62 Å. In the hydroxide layers, the Al–O

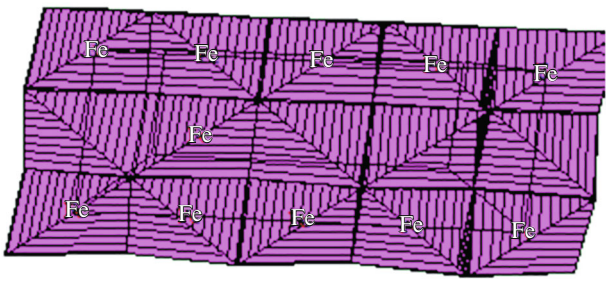

Fig. 3. FeS layer in the crystal structure of vyalsovite (projections on the (010) plane).

distances are slightly shorter than the Ca–O distances (2.06–2.28 Å and 2.32–2.51 Å, respectively). Due to the strong repulsion of Ca^{2+} and Al^{3+} cations, the divided octahedral edges are much shorter than the unseparated edges (a similar effect was observed in the structures of other minerals containing octahedral layers, e.g., in the structures of clay minerals). The S–OH interlayer contacts lie within 2.00–2.30 Å, which corresponds to the weak hydrogen bonds. The layered character of the structure and the weak interlayer interaction determine a finely dispersed character of vyalsovite precipitations and perfect cleavage on (010).

CONCLUSIONS

The crystal structure of natural hydrosulfide, vyalsovite $FeCaAlS(OH)_5$, composed of commensurate sulfide layers with octahedral coordination of Fe and hydroxide modules with one hydroxide layer, consisting of alternating octahedra, settled in an orderly manner by Ca^{2+} and Al^{3+} cations, was revealed for the first time.

FUNDING

This study was conducted under a State Assignment on the subject "Structural and Chemical Inhomogeneities and Paragenetic Associations of Minerals as Evidence of Petro- and Ore Genesis Processes," project no. 121041500220-0.

CONFLICT OF INTEREST

The authors declare that they have no conflicts of interest.

REFERENCES

1. G. Ferraris, E. Makovicky, and S. Merlino, *Crystallography of Modular Materials* (Kindle Edition, 2004).
2. H. T. Evans and R. Allmann, Z. Krist. **127**, 73–93 (1968).
3. N. I. Organova, *Crystal Chemistry of Disproportional and Modulated Mixed Layered Minerals* (Nauka, Moscow, 1989) [in Russian].
4. S. V. Soboleva, T. E. Evstigneeva, N. M. Boeva, and N. S. Bortnikov, Dokl. Earth Sci. **491** (2), 210–213 (2020). https://doi.org/10.1134/S1028334X20040182
5. T. E. Evstigneeva, A. D. Genkin, S. M. Sandomirskaya, and N. V. Trubkin, Am. Mineral. **77** (1), 201–206 (1992).
6. C. E. Tilley, Mineral. Mag. **23** (142), 419–420 (1933).
7. M. Russo and I. I. Punzo, *Minerali del Somma-Vesuvio* (Associazione Micro-Mineralogica Italiana, Tipografia Fantigrafica s.r.l, 2004).
8. C. Neal and G. R. Stanger, Mineral. Mag. **48**, 237–241 (1981).
9. E. Sokol, N. Volkova, and G. Lepezin, Eur. J. Mineral. **10** (5), 1003–1014 (1998).
10. V. E. Buchwald, Philos. Trans. R. Soc. London Math. Phys. Sci. **286**, 453–491 (1977).
11. A. I. Bakhtin, O. P. Shilovskii, and Yu. N. Osin, Uch. Zap. Kazan. Univ. Estestv. Nauki **156** (1), 174–181 (2014).
12. A. Kawohl and H. E. Frimmel, Mineral. Mag. **80** (6), 1041–1053 (2016).
13. R. H. Carpenter and G. A. Desborough, Am. Mineral. **49** (9–10), 1350–1365 (1964).
14. H. Saalfeld and M. Wedde, Z. Kristallogr. **139**, 129–135 (1974).
15. R. T. Mara and G. B. B. M. Sutherland, J. Opt. Soc. Am. **46** (6), 464–465 (1956).
16. H. T. Evans, Jr., in *Proc. 11th Apollo Lunar Sci. Conf.* (Houston, 1970), Vol. 1, pp. 399–408.
17. E. F. Bertaut, Bull. Soc. Fr. Mineral. Crystallogr. **79**, 276–292 (1956).
18. G. Ferraris, E. Belluso, A. Gula, and S. V. Soboleva, Can. Mineral. **39**, 1665–1667 (2001).
19. R. K. Rastsvetaeva, V. Zaitsev, and I. Pekov, Crystallogr. Rep. **65** (3), 434–440 (2020).
20. G. Ferraris, G. Ivaldi, A. P. Khomyakov, and S. V. Soboleva, Eur. J. Mineral. **8** (2), 241–249 (1996).

Translated by L. Mukhortova